

Novel nanocomposite of carbon nanotube–nanoclay by direct growth of nanotubes on nanoclay surface

M. LU*

School of Materials Science and Technology, Nanjing University of Aeronautics and Astronautics, Nanjing 210016, P. R. China; Department of Mechanical Engineering, The Hong Kong Polytechnic University, Hung Hom, Kowloon, Hong Kong, P. R. China
E-mail: lumei@lzu.edu.cn

K. T. LAU

Department of Mechanical Engineering, The Hong Kong Polytechnic University, Hung Hom, Kowloon, Hong Kong, P. R. China

J. Q. QI

Department of Materials Science & Engineering and State Key Laboratory of Fine Ceramics and New Processing, Tsinghua University, Beijing 100084, P. R. China

D. D. ZHAO, Z. WANG

College of Chemistry and Chemical Engineering, Lanzhou University, Lanzhou 730000, P. R. China

H. L. LI

School of Materials Science and Technology, Nanjing University of Aeronautics and Astronautics, Nanjing 210016, P. R. China; College of Chemistry and Chemical Engineering, Lanzhou University, Lanzhou 730000, P. R. China

Carbon nanotubes (CNTs), shown to possess outstanding characteristics of high Young's modulus, stiffness, and flexibility, hold high promises as reinforcement additives in composites for use in a wide range of applications [1–4]. At present, the generally adopted method for the mass production of CNTs is chemical vapor deposition (CVD), a relatively low cost method compared to others. The essential idea of the CVD method is the use of metal catalyst particles, i.e. Fe, Co, Ni, uniformly loaded on suitable supports such as zeolite, silica, alumina, MgO, *et al.*, with CNTs growth obtained by catalytic decomposition of hydrocarbon gases (methane, ethane, ethylene, acetylene) under optimal conditions [5–8]. However, with the exception of MgO, the removal of the support materials in the final steps of the CVD method is both tedious and difficult to achieve completely. The quality of the composite properties is negatively impacted without the complete removal of the support materials. To avoid this problem, Petridis *et al.* [9] attempted CNTs growth on the surface of clay with iron as a catalyst since clay itself is a good reinforcement for polymer-based composites with its high ion exchange capacity, high aspect ratio, ease of fabrication, and relatively low cost [10–13]. With the removal of the clay support, no longer being necessary, the peculiar CNTs–clay composite structure could be incorporated in the polymer matrix directly and the resulting composite is expected to exhibit enhanced mechanical properties combining the advantages of both CNTs and clay.

The work presented here will attempt a new catalyst/support preparation method by intercalating cobalt salt in the two-dimensional interlayer space of nanometer-sized clay. The following pH-controlled ion precipitation of cobalt cations by weak base will give rise to cobalt hydroxide particles in the interlayer space of nanoclay. Then Co(OH)₂/nanoclay hybrid was used to grow CNTs under reduced-pressure chemical vapor deposition conditions [14]. The predication is that the CNTs thus prepared would be protected from aggregation by the interlayer space of nanoclay. In addition, the degraded layered structure of nanoclay caused by CNTs growth within its interlayer spaces will be beneficial for the formation of mechanical interlocking between CNTs and nanoclay platelets as well as the future formation of exfoliated nanoclay in a polymer matrix. Compared to the conventional micro-sized clay fillers, addition of nanoclay in a polymer matrix has lead to nanocomposites exhibiting markedly improved physicochemical properties at lower loading. Accordingly, fabrication of CNTs–nanoclay would have more significance for the future generation of CNTs–nanoclay reinforced polymer composites.

An amount of 1.2 g cobalt acetate [Co(CH₃COO)₂ · 4H₂O] was dissolved in 100 ml of distilled water. An amount of 2 g of nanoclay was added to the cobalt acetate solution and allowed to sonicate for 4 hr. During the sonication, liquid ammonia was slowly titrated into the cobalt acetate–nanoclay mixture solution at different pH for Co(OH)₂ precipitation.

*Author to whom all correspondence should be addressed.

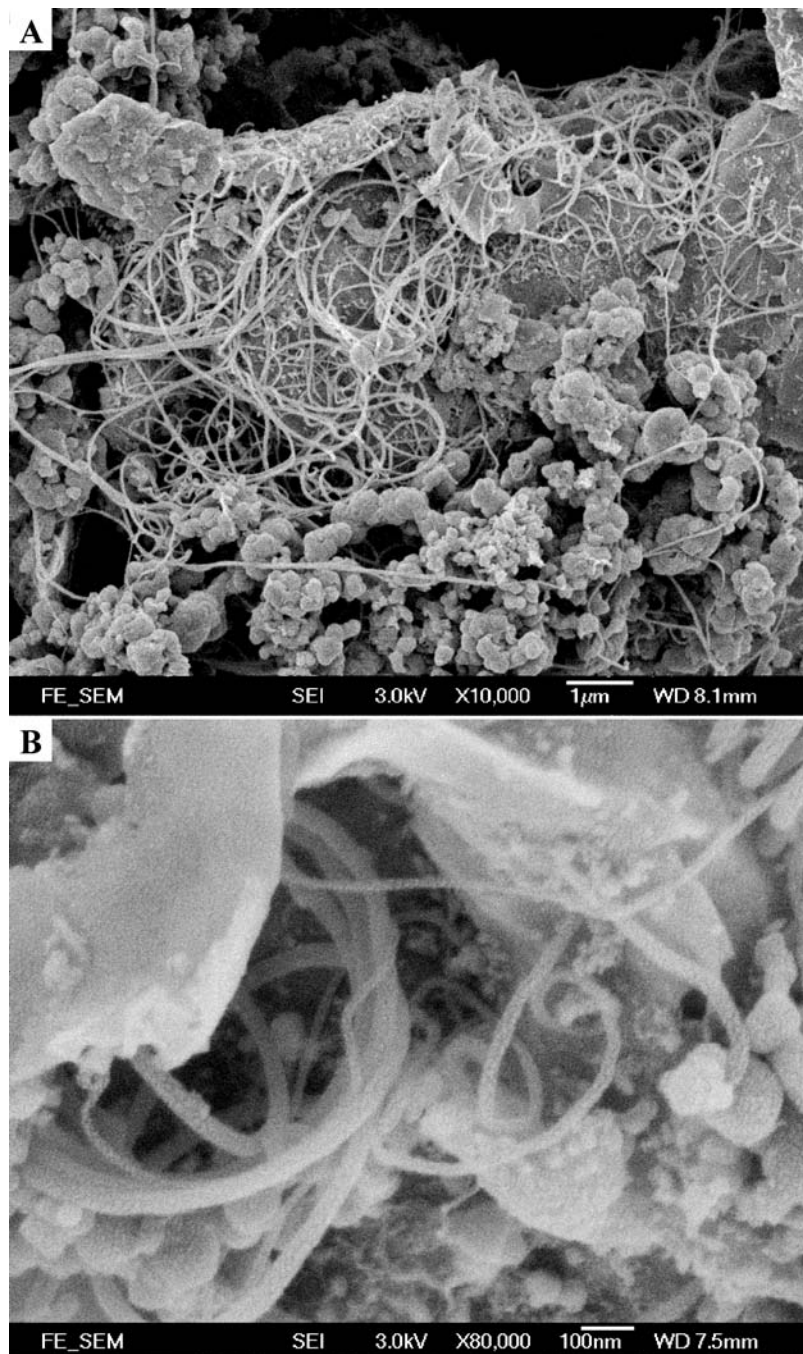


Figure 1 FE-SEM images of the morphology of CNTs–nanoclay composite at pH = 9.5 with high (A) and low (B) magnification.

After the precipitation, the mixtures were filtered and washed several times with deionized water. The prepared catalyst/support was then dried in the air overnight at 110 °C. The dried catalyst/support was ground to the form of fine powder for subsequent deposition. The catalyst/support was subjected to chemical vapor deposition at 720 °C under a base pressure of 100 Pa. Acetylene gas (C_2H_2) of 20 ml/min was flowed into the reactor for 30 min. Field emission scanning electron microscopy (FE-SEM, JSM 6335F NT) was used to analyze the morphology of the samples. TEM and HRTEM analyses were carried out with a JEOL-2010 microscope at an accelerate voltage of 200 kV. The X-ray powder diffraction (XRD) analysis was performed with a Philips X' Pert System using monochromatic $Cu K_{\alpha}$ radiation with a generator

voltage and current of 40 kV and 35 mA, respectively ($\lambda = 1.5406 \text{ \AA}$).

Figs 1A and 1B are the representative FE-SEM images for the CNTs produced from $Co(OH)_2$ –nanoclay hybrid at pH = 9.5 with low and high magnification. As shown in Fig. 1A, the produced CNTs are entangled with nanoclay within a large area and also dispersed in the nanoclay without any aggregation. Based on the high-magnification image in Fig. 1B, CNTs are observed to be protruding from nanoclay surfaces, indicating that the nanoclay layer precipitated by $Co(OH)_2$ particles indeed serves as a medium and allow for the CNTs growth. However, despite this observation, only a small quantity of CNTs growth are found in the sample of pH = 8.5, while nearly no CNTs growth can be observed in the sample with pH = 7.5. Since the

increase of OH^{-1} concentration (higher pH) can produce more $\text{Co}(\text{OH})_2$ colloidal particles to precipitate on the NC surface, which will result in more Co particles deoxidized from $\text{Co}(\text{OH})_2$ particles at high temperature, hence, more active sites on the NC surface for CNTs growth.

TEM image in Fig. 2A reveals pieces of nanoclay flakes co-existing in the field of observation in the sample of pH = 9.5. Each individual piece of nanoclay flakes are observed to serve as a growth-center for the CNTs that intertwine with other CNTs and ul-

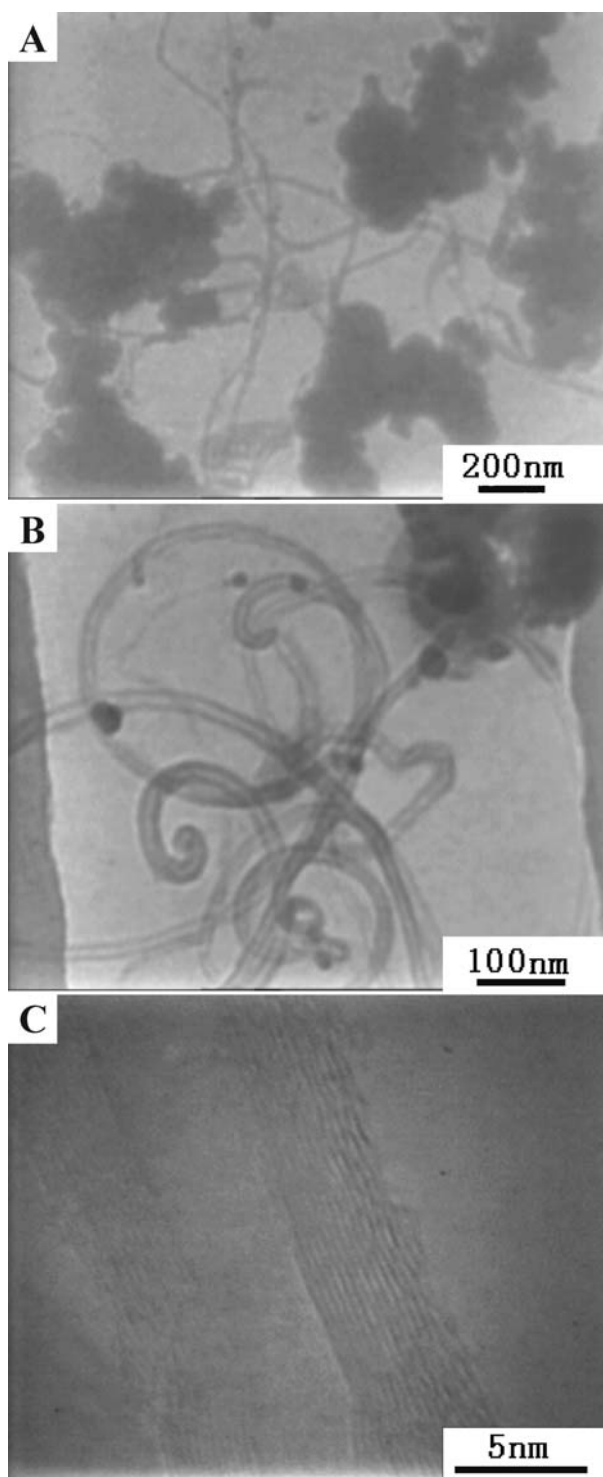


Figure 2 TEM images of several CNTs–nanoclay composite flakes (A) and the morphology of the produced CNTs at pH = 9.5 (B); HRTEM image of the tube wall of the produced CNTs at pH = 9.5.

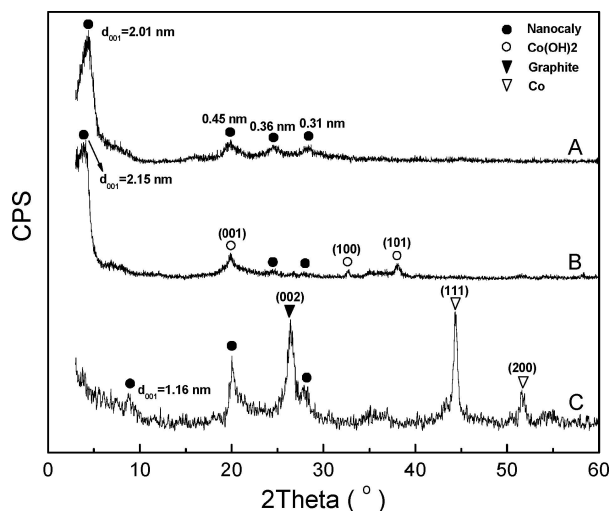


Figure 3 XRD patterns of pure nanoclay (A), $\text{Co}(\text{OH})_2$ –nanoclay hybrid produced at pH = 9.5 (B), and CNTs–nanoclay composite produced at pH = 9.5.

mately form an inter-network of structures between clay flakes. Fig. 2B indicates that the CNTs grown from the nanoclay layer indeed possesses a hollow-center structure with an average tube diameter of ~ 15 nm. The high-magnification TEM image (Fig. 2C) taken from a tube wall reveals an ordered graphitic structure of multi-walled tubes. The interlayer separation is approximately 0.334 nm and the tube wall thickness is about 4 nm, suggesting that the multi-walled CNTs consist of approximately 12 graphitic layers.

Changes in nanoclay structure brought about by catalyst particles precipitation and nanotubes growth are conveniently monitored by powder X-ray diffraction. Fig. 3 shows the powder XRD patterns of the samples at pH = 9.5 at different stages. The original d_{001} basal spacing of nanoclay was evidently expanded after $\text{Co}(\text{OH})_2$ precipitation from 2.013 to 2.149 nm. Since the surface of the negatively charged nanoclay is generally covered with charge compensating cations (Na^+ , Al^{3+} , etc.), which can be easily exchanged for other cations, the increase of the basal spacing of nanoclay should be due to the intercalation of Co^{2+} and cationic Co-amino complex into the interlayer space of nanoclay. In addition, the peak of the (001) reflection in the pattern B is not as sharp as that in the pattern a for the pure nanoclay, implying that the precipitated $\text{Co}(\text{OH})_2$ particles on the nanoclay surface can lead to the formation of a weakly ordered layered structure in nanoclay. In pattern B, the diffraction peaks of brucite-like phase of $\text{Co}(\text{OH})_2$ at $2\theta = 19.9^\circ$, 32.6° , and 38.0° , namely (001), (100), and (101) can also be observed [15].

After the growth of CNTs, the (001) peak characteristic of nanoclay disappears in pattern C, revealing that the process of high-temperature growth of CNTs has resulted in a collapsed state of the clay layers. TEM results have revealed that CNTs produced from nanoclay layers entangled with each other and formed a network structure within the nanoclay layer spacing. As a result, the nanoclay layers could dislocate from their original crystal lattice with nanotube pulling in different direction, which may disrupt the highly ordered parallel

layered structure of nanoclay. In addition, the non-basal reflections of nanoclay at 0.446 and 0.314 nm are still present in pattern C, indicating that the basic structure of the nanoclay is changed post CNTs formation instead of being destroyed. Therefore, a more accurate statement is that the nanoclay structure in the XRD pattern shows degradation after the CNTs growth. In pattern C, the presence of graphite (002) peak at $2\theta = 26.5^\circ$ corresponds to the diffraction characteristics of the parallel cylindrical graphite shells of CNTs. The average d_{002} interlayer spacing of CNTs is estimated to be 0.3361 nm by applying the Bragg equation, which is consistent with that calculated from TEM image. It is also noticed that in the (111) and (200) reflections of Co in pattern C, there is an indication that $\text{Co}(\text{OH})_2$ particles have been reduced to Co catalytic particles at high temperature for CNTs growth.

In summary, using nanoclay as a support material, we present a method to prepare novel CNTs–nanoclay composite by direct growth of CNTs on the nanoclay surface. Electron microscopy showed the formation of a three-dimensional network structure between CNTs and nanoclay under the optimal pH value. XRD results proved the expanded nanoclay layers after the precipitation of $\text{Co}(\text{OH})_2$ particles and the degradation of nanoclay structure after CNTs growth. The novel CNTs–nanoclay composite reported here holds high potential for application as electrochemical materials, polymer reinforcements, and other functional materials. The actual use will be apparent as the precise physical and mechanical properties of the composite become available through planned future studies.

Acknowledgments

This work is partly supported by The Hong Kong Polytechnic University Grants (G-T 861 and G-T 936).

References

1. L. S. SCHADLER, S. C. GIANNARIS and P. M. AJAYAN, *Appl. Phys. Lett.* **73** (1998) 3842.
2. M. CADEK, J. N. COLEMAN, V. BARRON, K. HEDICKE and W. J. BLAU, *ibid.* **81** (2002) 5123.
3. H. Z. GENG, R. ROSEN, B. ZHENG, H. SHIMODA, L. FLEMING, J. LIU and O. ZHOU, *Adv. Mater.* **14** (2002) 1387.
4. S. BARRAU, P. DEMONT, E. PEREZ, A. PEIGNEY, C. LAURENT and C. LACABANNE, *Macromolecules* **36** (2003) 9678.
5. L. F. SUN, J. M. MAO, Z. W. PAN, B. H. CHANG, W. Y. ZHOU, G. WANG, L. X. QIAN and S. S. XIE, *Appl. Phys. Lett.* **74** (1999) 644.
6. J. E. HERRERA and D. E. RESASCO, *J. Phys. Chem. B* **107** (2003) 3738.
7. K. HERNADI, Z. KONYA, A. SISKA, J. KISS, A. OSZKO, J. B. NAGY and I. KIRICSI, *Mater. Chem. Phys.* **77** (2003) 536.
8. J. F. COLOMER, C. STEPHAN, S. LEFRANT, G. VAN TENDELOO, I. WILLEMS, Z. KONYA, A. FONSECA, C. LAURENT and J. B. NAGY, *Chem. Phys. Lett.* **317** (2000) 83.
9. D. GOURNIS, M. A. KARAKASSIDES, T. BAKAS, N. BOUKOS and D. PETRIDIS, *Carbon* **40** (2002) 2641.
10. H. KOERNER, J. D. JACOBS, D. W. TOMLIN, J. D. BUSBEE and R. A. VAIA, *Adv. Mater.* **16** (2004) 297.
11. D. SHAH, P. MAITI, E. GUNN, D. F. SCHMIDT, D. D. JIANG, C. A. BATT and E. P. GIANNELIS, *ibid.* **16** (2004) 1173.
12. P. VIVILLE, R. LAZZARONI, E. POLLET, M. ALEXANDRE and P. DUBOIS, *J. Amer. Chem. Sci.* **126** (2004) 9007.
13. L. S. LOO and K. K. GLEASON, *Macromolecules* **36** (2003) 2587.
14. M. LU, H. L. LI and K. T. LAU, *J. Phys. Chem. B* **108** (2004) 6186.
15. Z. P. XU and H. C. ZENG, *Chem. Mater.* **11** (1999) 67.

Received 9 November

and accepted 20 December 2004